1-1-2014

A force sensing tool for disassembly operations

Paul Schumacher
Sensata Technologies, Inc.

Musa Jouaneh
University of Rhode Island, jouaneh@uri.edu

Citation/Publisher Attribution

Schumacher, Paul, and Musa Jouaneh. "A force sensing tool for disassembly operations." *Robotics and Computer-Integrated Manufacturing* 30, 2 (2014): 206-217. doi: 10.1016/j.rcim.2013.09.016.

A force sensing tool for disassembly operations

Keywords

Disassembly tool; End of life electronics; Force sensing resistors; Robotic disassembly

P. Schumacher, and M. Jouaneh, "A Force Sensing Tool for Disassembly Operations," Robotics and Computer-Integrated Manufacturing, Vol. 30, No. 2, pp. 206-217, 2014.

A Force Sensing Tool for Disassembly Operations

Paul Schumacher[1] and Musa Jouaneh
Department of Mechanical, Industrial, and Systems Engineering
University of Rhode Island
Kingston, RI 02881

Abstract

This paper discusses the design and characterization of a prototype disassembly tool that was designed to handle a family of electronic devices whose plastic, cantilever snap-fit covers house AA or AAA batteries. The tool was designed with the ability to release the snap-fit covers and the batteries contained inside. The tool design is based on the use of a force sensing tool tip that utilizes three force sensing resistors (FSRs) for force feedback. Two FSRs were used to measure horizontal forces applied to the tool tip while the third FSR was used to measure forces along a direction normal to the tool tip. The tool tip is used to push and lift up the snap-fit cover as well as the spring-loaded batteries. By using the conductance of the FSR sensors, a linear model of the FSR output was calibrated to the force applied to the FSR. The disassembly tool was mounted on a three-axis translational motion robot, and the robot was programmed to perform disassembly operations. Sensor feedback from the FSRs was used to control the movement of the tool during these operations. The results showed that the robot was able to successfully use the disassembly tool to perform the necessary operations to remove the device's snap-fit cover and batteries. Force readings recorded from the FSRs indicated that the disassembly tool was able to react to force interactions at the disassembly tool tip such as a missing part or misaligned part. The use of FSRs resulted in a low-cost, flexible disassembly tool.

Keywords: Disassembly tool, force sensing resistors, robotic disassembly, end of life

[1] Currently at Sensata Technologies, Attleboro, MA

electronics.

I. Introduction

Automated disassembly of end of life electronic products has been receiving considerable attention [1-4]. Due to the vast variety and conditions of electronic products, special tools are required for efficient disassembly. Several researchers have investigated the design of disassembly tooling and grippers. Rebafka et al. [5] proposes a flexible unscrewing tool that creates its own acting surfaces in order to improve loosening. Park and Kim [6] discuss the development of a 6-axis force/moment sensor for an intelligent robot's gripper. In addition, Feldmann et al. [7] details the design of a so called drilldriver, which can be used for three different methods of disassembling joining members: use an existing working point to remove a fastener, drill to create a working point to remove a fastener, or drill to destroy the joint. Zuo et al. [8] also presents a novel disassembly tool, wherein a screwnail is used as an end effector. A self-connection resulted from the screwnail indentation provides a reliable closure to transmit forces and torques required for various dismantling operations. Weigl and Seitz [9] outline the development of a three-fingered dexterous gripper with three joints per finger which combines with a six-axes robot arm to create a highly redundant coordinated hand-arm-system. The increased flexibility of this hand-arm-coordination allows dexterous manipulations necessary for complex and skillful disassembly operations. O'Shea et al. [10] proposes a method for the automatic selection of tools in a disassembly environment. The method uses a dynamic programming model that produces an optimum tool selection path. El-Sayed et al. [11] discuss a sequnece generator for robotic disassembly of end of life electronic products.

These studies clearly indicate the need for adaptive tooling to be developed for successful automated disassembly. One of the major issues in dealing with end of life electronics is the

immense variety of products. Designing a system with intricate tooling that can only disassemble one type of device or just a specific brand of product within that device type is expensive and inefficient. In order for automated disassembly to be successful and profitable, the systems must be designed to be versatile and adaptable to a variety of products. The goal of this project was to design an intelligent, automated tool that can perform a disassembly task common to a variety of electronic devices. Snap-fit fasteners are very common in the design of electronic devices, especially in the outer plastic housings. The release of plastic snap-fit covers is a highly routine procedure needed for the removal of external housings in order to make accessible the internal components of an electronic device. During assembly snap-fit components are merely oriented and pushed into place, which is a simple process requiring basic manipulation. In comparison, during disassembly the cantilever of the snap-fit must be disengaged while simultaneously pulling or sliding the component out of the assembly. Disengaging snap-fits requires a special tool and more sophisticated coordination. In this paper, a flexible, force-based disassembly tool that uses FSRs for force sensing was designed for the purpose of removing exterior plastic snap-fit covers on electronic devices and then recovering the hazardous batteries enclosed within. Designing such an adaptive tool is a step towards more flexible and efficient automated disassembly systems.

FSRs were chosen for development in the tool because they are small, lightweight, and low-cost. FSRs have been used in a number of force sensing applications. Nikonova et al. [12] describes a system that measures forces over the entire hand using thin-film FSRs. The system has been successfully used to measure forces involved in a range of everyday tasks such as driving a vehicle, lifting a saucepan, or hitting a golf ball. In Smith et al. [13], FSRs were used to detect the transitions between five main phases of gait for the control of electrical stimulation

while walking with several children with cerebral palsy. FSRs have also been used in a number of simple touch applications. Several patents describe the integration of FSRs as simple touch sensors for a variety of devices including: a controller apparatus [14], pointing device [15], keyboard [16], and three-dimensional mouse [17].

The remainder of this paper is organized as follows. Section II gives the initial design considerations for such a tool. Section III discusses the characterization of the force sensing resistors used in the design. The prototype design of the tool is discussed in section IV. Section V illustrates the disassembly operations, while Section VI discuses the force sensor results. Section VII discusses a tool for internal snap-fits. The concluding remarks are given in Section VIII.

II. Initial Design Considerations

The disassembly operations required by the tooling are as follows: (1) Release a cantilever snap-fit fastener (2) Remove and discard the plastic snap-fit cover (3) Release the batteries contained within the electronic device (4) Remove and dispose of the batteries. The disassembly module also needed to be designed within the constraints of a 3-axis robotic platform used for testing the tool. The robot has three translational degrees of freedom and a pneumatic system equipped with both solenoid valves and vacuum pumps.

It was first necessary to determine the approximate force needed to compress a snap-fit lever. The force required to compress a snap-fit depends both on its material and geometric parameters. Therefore, it was decided to design for the maximum force that a typical electronic device's snap-fit could require. A number of different small electronic devices were sampled and the device that clearly had the stiffest snap-fit was a TI-84 calculator. Thus, the TI-84 calculator's snap-fit was analyzed to determine the approximate force range necessary for

release. The force to compress the snap-fit was calculated using analytical equations based on classical beam theory and obtained from plastic snap-fit guides [18-19].

These analytical solutions were used to calculate the force necessary to deflect the typical U-shaped cantilever snap-fit of the TI-84 calculator. The analytical equations used to model the U-shaped snap-fit are shown below in Figure 1.

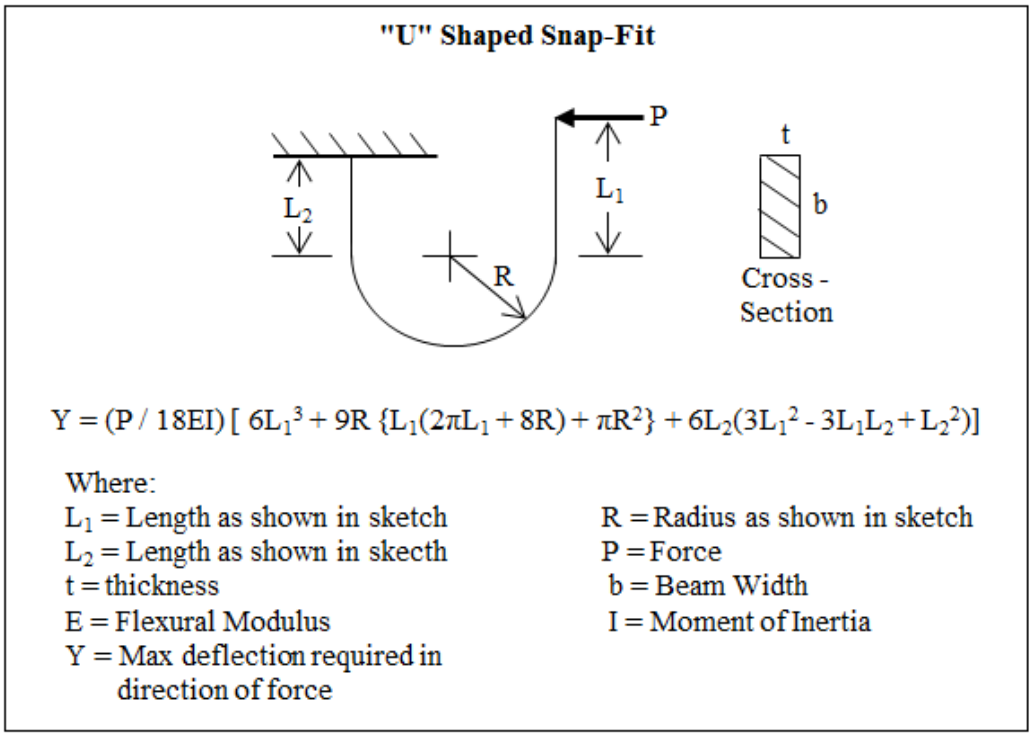

Figure 1: "U" Shaped Analytical Snap-Fit Equations

The necessary geometric parameters of the T-84 Calculator were measured using vernier calipers and are listed here: R = 1.778 mm (0.07”), L_1 = 8.0 mm (0.315”), L_2 = 7.112 mm (0.280”), t = 1.143 mm (0.045”), b =19.431 mm (0.765”), Y = 3.81 mm (0.150”), and I = 2.418 mm^4 (5.809x10-6 in^4). The material of the snap-fit is an ABS / Polycarbonate (PC) mix. Since PC is slightly stiffer than ABS, the modulus of elasticity of PC (2585.5 MPa or 375 ksi) was selected. Plugging into the equation pictured in Figure 1, a deflection force of 20.6 – 29.5 N (4.63 - 6.62 lbs) was calculated for the snap-fit. A range of forces was computed in order to

include the possible human errors in measuring the snap-fit geometries and the inability to determine the exact composition of its material.

In designing the tool, a means to monitor the force interactions needed to be established. Load cells were determined to be unsuitable for this application due to their relatively large size and high cost. Force sensing resistors (FSRs) were chosen for development in the tool because they are small, lightweight, and low-cost. While load cells are more durable and can provide a greater range for accurate force measurement, they can cost hundreds to thousands of dollars. In this application, force measurements on multiple axes of motion are required. Thus, either a single, multi-axis load cell would be required or multiple loads cells oriented to read force measurements on different axes, further increasing the potential cost of using load cell technology. In comparison, FSRs cost $5 to $20 depending on the supplier and the force range. Therefore, FSRs were determined to be more suitable for the development of a low-cost tool where only relatively small forces must be measured. The next section describes the theory behind the FSRs and the process used to characterize these force sensors.

III. Characterization Of Force Sensing Resistors

FSRs are paper-thin, flexible printed circuits that sense contact forces. When the sensor is unloaded, its resistance is very high so no voltage passes through the circuit. When a force is applied to the sensor, the resistance decreases and a voltage passes across the circuit [20]. The voltage across the circuit can be measured and calibrated to units of force. The most basic FSR consists of two membranes separated by a thin air gap. A conductive material is applied to one layer and pressure-sensitive ink is applied to the other layer. When the two substrates are pressed together, the microscopic protrusions on the FSR ink surface make connections across the active sensing area, allowing current to flow between the conductive leads [21]. At low forces only the

tallest ink protrusions make contact, and as the force increases more and more points make contact and increase the current flow. Thus, resistance between the conducting leads decreases as the force increases. A FSR is commonly used by connecting one end to a power supply and the other to a pull-down resistor to ground [21]. Then the voltage output at the point between the fixed pull-down resistor and the variable FSR is used as the output of the FSR. A diagram of such a circuit is illustrated in Figure 2 and an equation for the voltage output of the FSR circuit is shown in Equation 1.

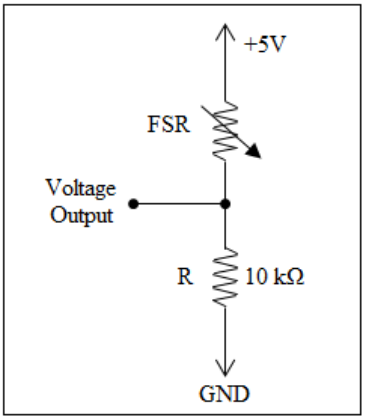

Figure 2: FSR Analog Voltage Reading Circuit

$$V_{OUT} = V_{IN}\left(\frac{R}{R + R_{FSR}}\right) \quad (1)$$

As the resistance of the FSR decreases, the total resistance of the FSR and the pull-down resistor decreases. The decrease in resistance means that the current flowing through both resistors increases and in turn causes the voltage across the fixed resistor (R) to increase. In Figure 2 the fixed resistor is a 10 kΩ resistor. However, the value of the fixed resistor can be changed to manipulate the sensitivity and range of the force sensor readings. A higher reference resistance will make the sensor more sensitive and decrease its active force range.

As mentioned earlier, FSRs are typically used in simple touch applications rather than to accurately measure force variations. Thus, three different FSRs were tested to determine if they were a viable option for measuring the force interactions of the disassembly tool. The three FSRs

tested were a FlexiForce Sensor and two different Interlink Electronics FSRs. All of the force sensors have a maximum load capacity of approximately 111 N (25 lbs); however, each FSR has a unique sensing area diameter. The FlexiForce sensor has a sensing area diameter of 0.375” and the Interlink FSRs have a sensing area diameter of 0.5” and 0.2”. The three FSRs are pictured in Figure 3.

0.375” FlexiForce FSR **0.2” Interlink FSR** **0.5” Interlink FSR**

Figure 3: Images of FSRs Tested

In order to characterize the sensors, each was loaded with a set of fixed weights and the voltage was measured at the known weight increments. A force vs. voltage plot was then created to visualize the response of each sensor. Due to the characteristics of the pull-down resistor circuit, the reference resistor could be varied to change the sensitivity and range of the sensor. The recommended resistance of the fixed resistor is a range from 1 kΩ to 100 kΩ [20]. Thus, the value of the fixed resistor was varied for each sensor in 10 kΩ increments to determine the reference resistance that produced the best combination of sensitivity and range. The results of the force sensor characterization are shown in Figures 4 and 5. Since the response of the two Interlink FSRs was comparable, only one force plot is displayed to represent the characterization of both sensors.

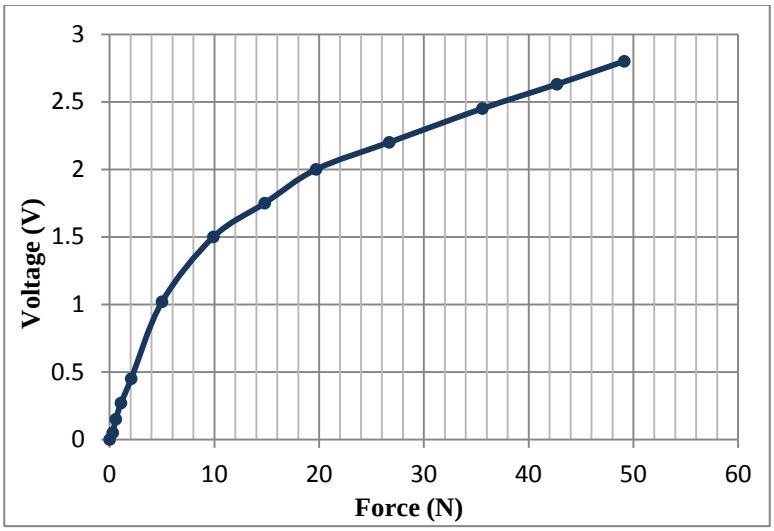

Figure 4: 0.375" FlexiForce FSR - Force Characterization Plot (R=80 kΩ)

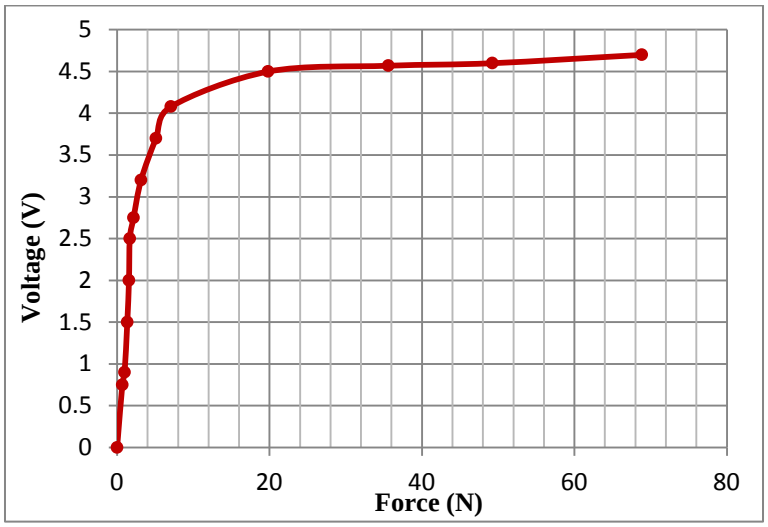

Figure 5: 0.2" & 0.5" Interlink FSRs - Force Characterization Plot (R=10 kΩ)

Figure 5 shows that the Interlink FSRs are too sensitive for measuring forces accurately. A small fixed resistance of 10 kΩ was used and the sensor still produced a highly non-linear response that almost completely saturates at 25 N of force. Thus, the sensitivity and the range were unsuitable for the disassembly tool application. On the other hand, the FlexiForce FSR showed more promising results. While the response is still non-linear, the sensitivity of this FSR provides a more even distribution of the voltage readings. The force range of the FlexiForce FSR also exceeds the desired 50 N range needed for the disassembly tool. Therefore, it was

determined that the FlexiForce sensor could be used to measure forces to provide feedback control of the disassembly tool. The reason the FlexiForce FSR is able to measure forces at a higher range more accurately than the Interlink FSRs is because it has a higher internal resistance. The FlexiForce FSR has an internal resistance of 5MΩ compared to the 1MΩ internal resistance of the Interlink FSRs.

IV. Prototype Design

Once it was determined that an FSR could be used to provide force feedback for control, a design concept was developed to integrate these sensors into the disassembly tool. A sketch of the design concept is illustrated in Figure 6.

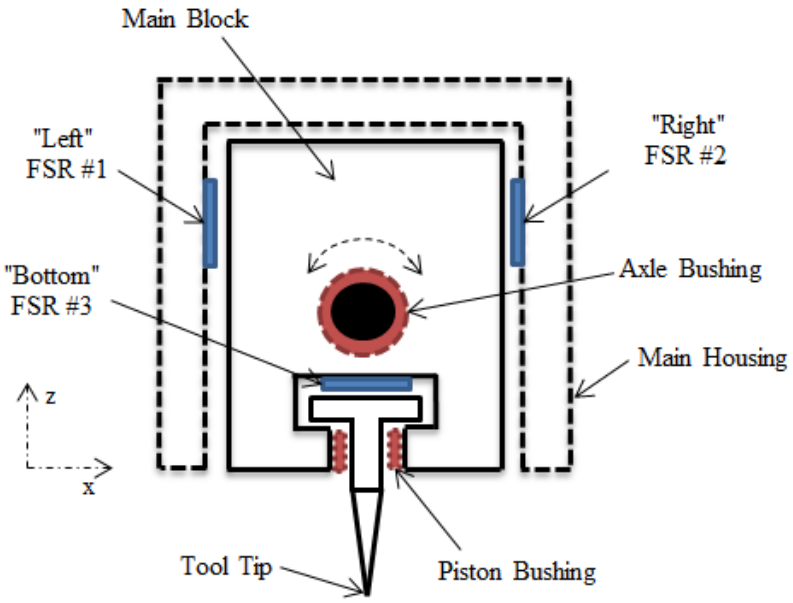

Figure 6: Design Concept Sketch

The basic concept of this design was to create a force sensing tip that could unfasten the snap-fit utilizing the x-y-z translational motion of a robotic platform. The tool is equipped with three FSRs to detect horizontal forces applied to the tool tip along the x-axis and to detect vertical forces applied to the tool tip along the z-axis. When a horizontal force is applied to the tip, the main block swivels and touches an FSR located inside the main housing. Likewise, when

a vertical force is applied to the tool tip, it slides up in the bushing and touches the FSR in the main block. The tool functions by moving to the snap-fit location and then moving the tip down until it contacts the surface of the electronic device. When the tip touches down, the FSR in the main block will register the vertical force and signal the tool to stop moving in the z-axis. Then the tool will move in the x-axis and push the snap lever with the tool tip until it is fully deflected. The tool knows when the snap-fit is fully deflected by monitoring the force readings of the appropriate FSR in the main housing. The tool then moves up in the z-axis releasing the snap-fit. Again, the tool recognizes when the snap-fit is unfastened because the force read by the FSR will decrease to zero as the snap-fit is released. Another important aspect of this design concept is that the same disassembly routine used to unfasten the snap-fit can also be applied to releasing the batteries. In the case of the batteries, the tool tip is inserted on the edge of the battery opposite the spring. The tool then pushes the battery, compressing the spring. Once the spring is compressed, the tool moves up in the z-axis releasing the battery. A SolidWorks model of the disassembly tool is pictured in Figures 7 and 8.

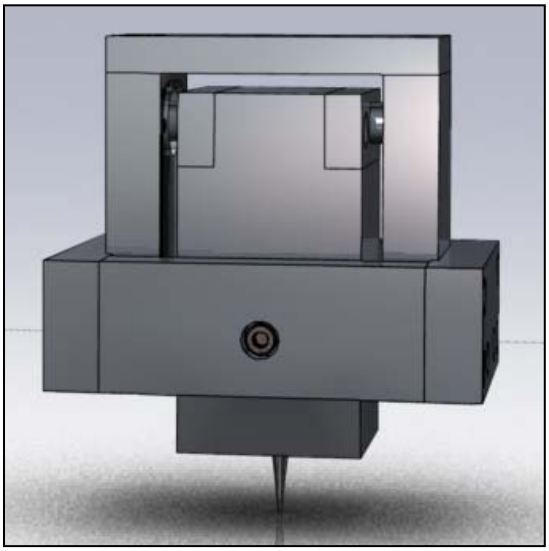

Figure7: SolidWorks Model

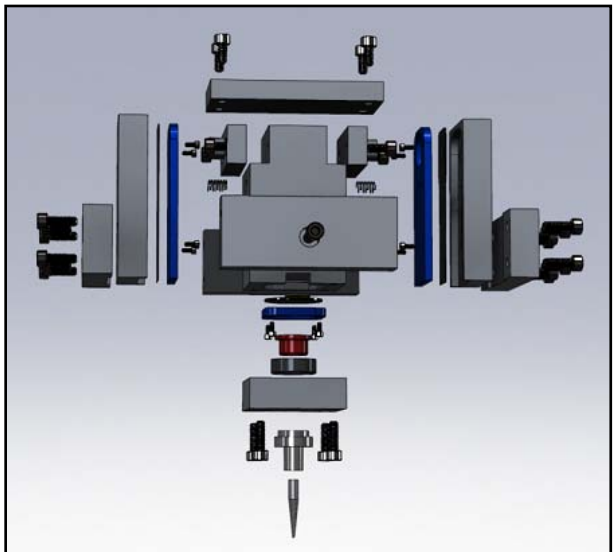

Figure 8: SolidWorks Model Exploded

Since most snap-fits have a protruding edge at the end of the snap lever, it was thought that a small hook at the end of the tool tip rather than a point could aid in releasing the snap-fit by catching this protruding edge. However, this leads into another important design consideration in that the tool must be able to release both the snap-fit and the batteries. A hooked tool tip would cause issues when dealing with the release of the batteries due to its shape and space constraints. Therefore, the tool tip was designed with a cone shape so that it may adapt to both the removal of the snap-fit and batteries.

Two FlexiForce sensors are used to measure the force applied to the tool tip in the positive and negative x-directions. A 0.5" Interlink FSR is housed inside the main block to detect vertical forces in the tool tip along the z-axis. Since the main block swivels and contacts the housing plate at a slight angle, the surface of the cylindrical force applicators is tapered in such a way that it presses flat against the housing plate. The detailed design of the tool is described in [22].

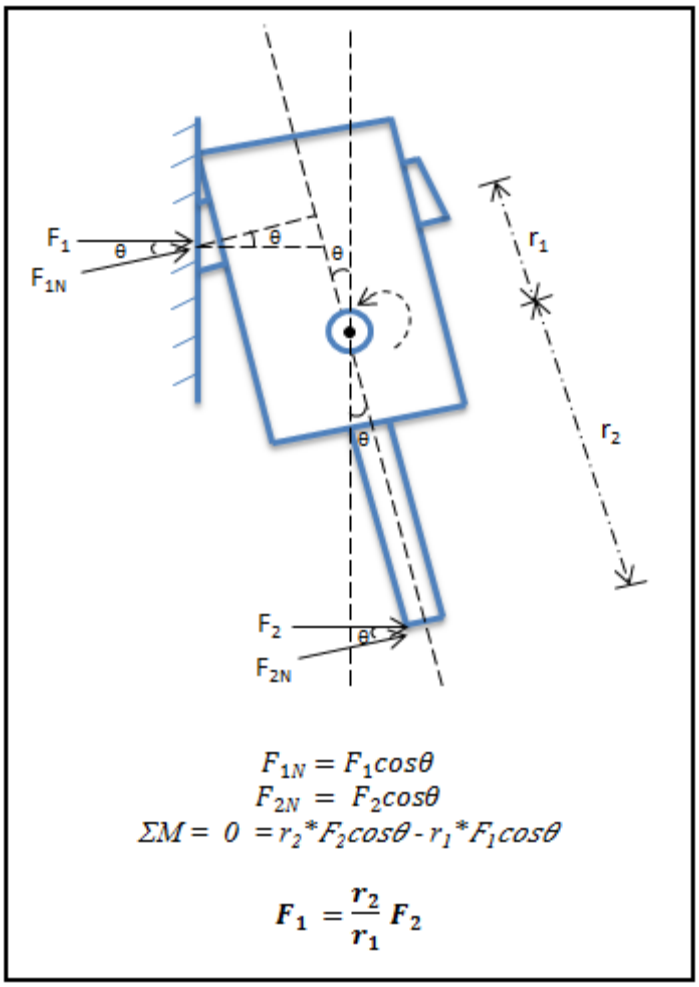

Figure 9: Force Relationship Diagram

An important parameter to consider in the design of the tool was the length of the main block and the tool tip. The main block swivels on an axle and therefore must be treated as a lever arm system. The length from the axle to the end of the tool tip (r_2) and the length from the axle to where the main block contacts the force sensor (r_1) greatly affect the relationship between the force applied to the tool tip and the force measured by the FSR. The relationship between the force applied at the tool tip (F_2) and the force measured by the force sensor (F_1) is demonstrated in Figure 9.

A 1:1 ratio was determined to be the desired length ratio for the lever arm system due to the resolution and range of the FSRs. As a result, the design of the prototype is somewhat "bulky" because of the need to increase the length of the main block in order to create the 1:1 lever arm ratio. The width and thickness of the main block were made as small as possible while still being able to house the 0.5" Interlink FSR and fastening bracket. A picture of the completed prototype build is shown in Figure 10.

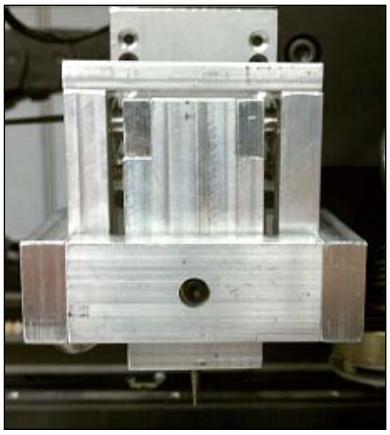

Figure 10: Prototype Build

The FSR1 ("left) and FSR2 ("right") sensors needed to be recalibrated while mounted inside the actual prototype to reduce the friction and compliance errors. The FSRs were calibrated using a digital force gauge. The digital force gauge was used to push the tool tip in the appropriate direction and a force versus voltage relationship was recorded. From this relationship, an equation could be fit to the data in order to describe the force in terms of the voltage read by the FSR. The calibration process is now illustrated in more detail for FSR1 in order to show how both FSR1 and FSR2 were calibrated. First, the voltage versus force response is plotted below in Figure 11.

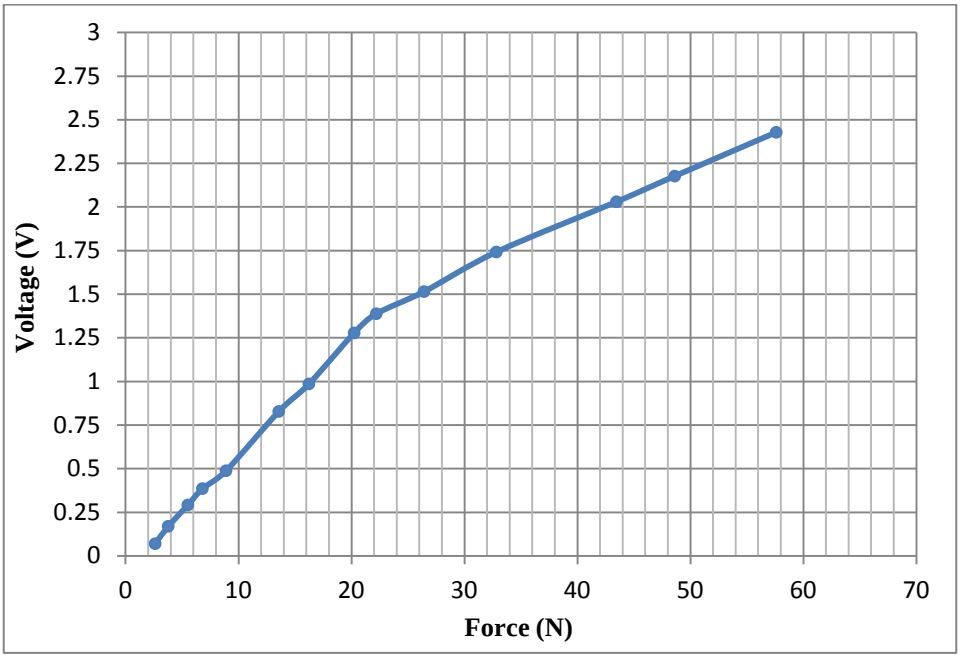

Figure 11: FSR1 - Voltage vs. Force Plot (R = 80kΩ)

As Figure 11 indicates, the voltage response is non-linear and would be difficult to accurately fit an equation to. However, through a simple derivation, the conductance (1 / Resistance) can be plotted as a function of the applied force, which produces a more linearized result [20]. In order to plot the conductance, the resistance of the FSR must first be calculated. Solving for the resistance of the FSR in Equation 1, the following relationship is derived:

$$R_{FSR} = \frac{R(V_{IN} - V_{OUT})}{V_{OUT}} \qquad (2)$$

where R is the fixed resistance and R_{FSR} is the variable resistance of the FSR. To solve for the conductance, the FSR resistance is simply inverted. The conductance versus force plot is shown in Figure 12.

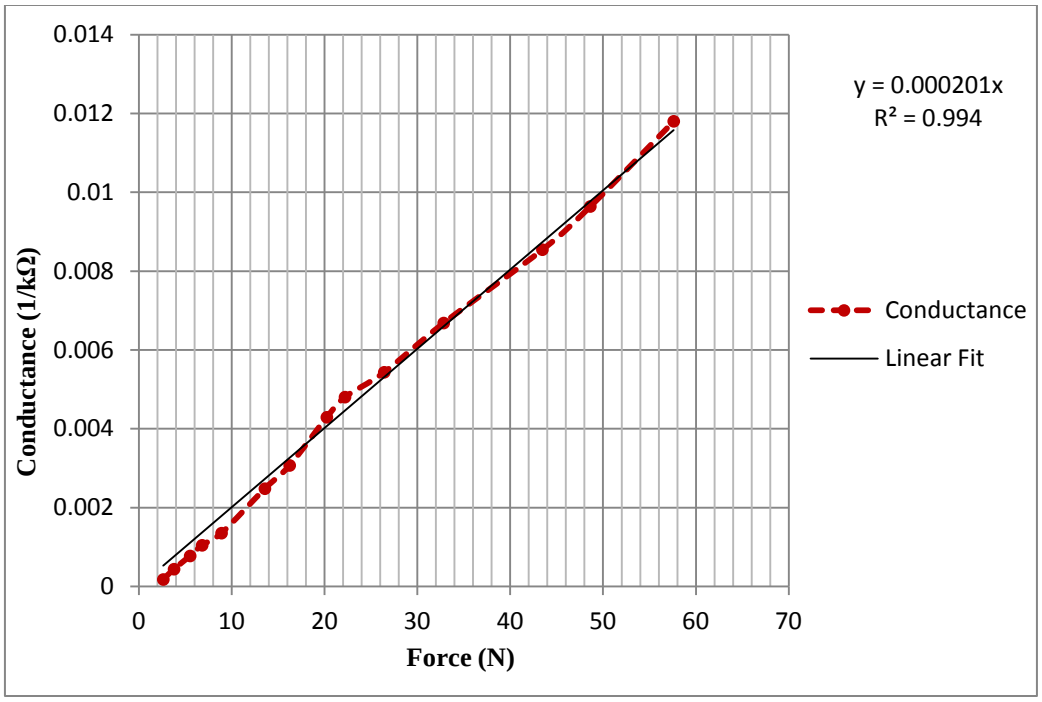

Figure 12: FSR1 - Conductance vs. Force Plot

Using the equation of the linear fit line in Figure 12, the following relationship describes the force measured by the FSR as a function of conductance.

$$FORCE_{FSR} = 4980 * C \quad (3)$$

Since the conductance is a function of the FSR's resistance and the resistance is a function of the FSR's voltage output, an equation for the force measured by the FSR as a function of the voltage output can be derived as follows:

$$FORCE_{FSR} = 4980 * \left(\frac{1}{R_{FSR}}\right) \quad (4)$$

Substitute Equation 2 into Equation 4.

$$FORCE_{FSR} = 4980 * \left(\frac{V_{OUT}}{R(V_{IN} - V_{OUT})}\right)$$

$$FORCE_{FSR} = 4980 * \left(\frac{V_{OUT}}{80(5V - V_{OUT})}\right) \quad (5)$$

Figure 13 below is a plot comparing the actual force response of FSR1 to the model derived in Equation 5.

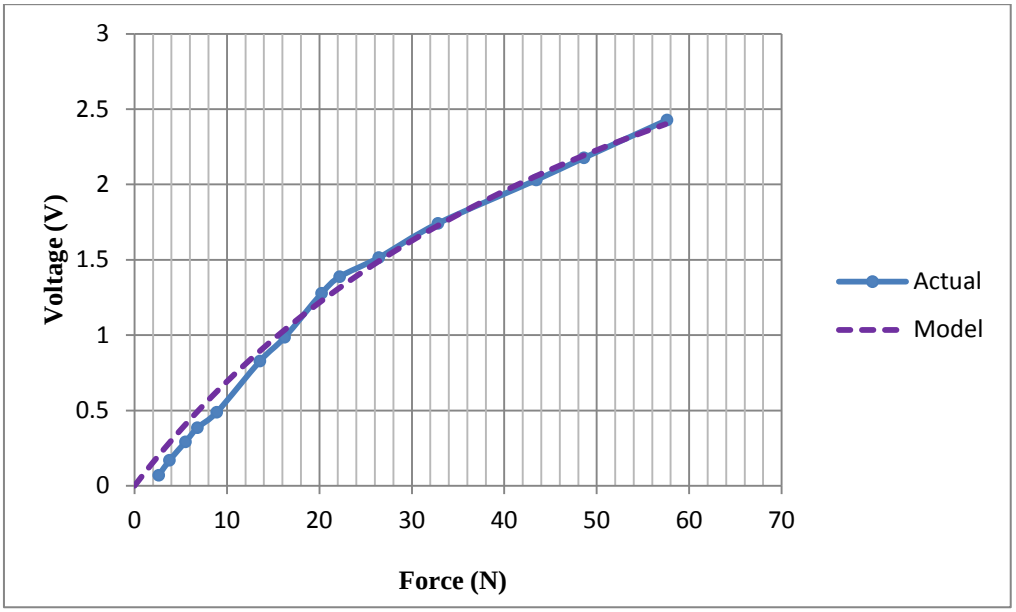

Figure 13: FSR1 - Actual vs. Model Comparison Plot

The comparison plot of Figure 13 shows that the model is a good approximation of the actual force measured by the FSR. There is a slight variation between the actual response and the model between 0 and 15 N, which is most likely due to the way in which the force at the tool tip is transferred through the moment arm before it is measured by the FSR. As the moment arm swings, the tool tip must move a small distance before the force applicator makes contact with the FSR. During this interval where the moment arm swings and before it makes contact with the FSR, no force is measured by the FSR despite there being a small force applied at the tool tip.

Due to the high non-linearity and poor resolution of the Interlink FSRs, the conductance derivation did not produce a linear model as in the FlexiForce calibration. Since the Interlink sensors are only used as simple touch sensors, the force characterization is not as vital to the function of the prototype as it was in the FlexiForce sensors. Furthermore, as simple touch sensors; the Interlink FSRs should only experience brief, small forces because the direction of

the tool head is reversed upward as soon as these sensors measure a slight increase in force. Therefore, it was decided to approximate the force measured by the Interlink FSRs by splitting the force response plot of Figure 5 into two linear segments. As shown in Figure 5, the voltage output is approximately linear up to 4.25 volts, and then after a small non-linear segment becomes approximately linear again with a different slope than the first linear segment. Therefore, a linear fit was applied to these two segments and a simple "if" statement was used to determine which linear fit equation to use to approximate the force. If the voltage read by the FSR is less than 4.25 volts then the slope for the first segment is used to approximate the force, and if the voltage read by the FSR is greater than 4.25 volts then the slope of the second segment is used to approximate the force. The slope for the first linear segment was determined to be .58 (V/N) or 1.7 (N/V) and the slope for the second linear segment was determined to be 0.0040 (V/N) or 250 (N/V). This technique was used to approximate the vertical force applied to both FSR3 and FSR4.

V. Illustration Of Disassembly Routine

In order to perform the necessary disassembly operations, the force sensing tool was mounted on a three-axis, linear motion robot, which is shown to the right in Figure 14. In addition, a vacuum gripper was mounted on the robot's tool head for retrieving the snap-fit covers once they are released and an electromagnet recovery system was also added for removing the batteries. A computer vision application was also implemented by mounting a Kinect for Windows sensor above the robot base and using the OpenCV library to process the

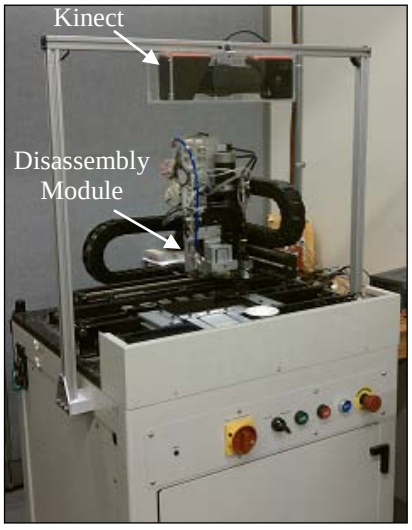

Figure 14: Complete Disassembly System

Kinect's RGB and IR data streams. The computer vision application uses a matching function to identify the electronic device and localize it in the image frame. Once the robot has gathered this information, it is able to look up the matched device's parameters and make the necessary coordinate transformations to calculate the position of the snap-fit and the batteries. Next the disassembly tool moves in the x-y plane to the location of the snap-fit. The tool is then moved down in the z-axis until it contacts the device's surface, at which point the tool tip is moved in the appropriate direction to deflect the snap lever. Once the tool detects the snap lever is fully compressed from reading the force sensor feedback, the tool moves up in the z-axis to release the snap-fit. Figure 15 depicts these disassembly operations.

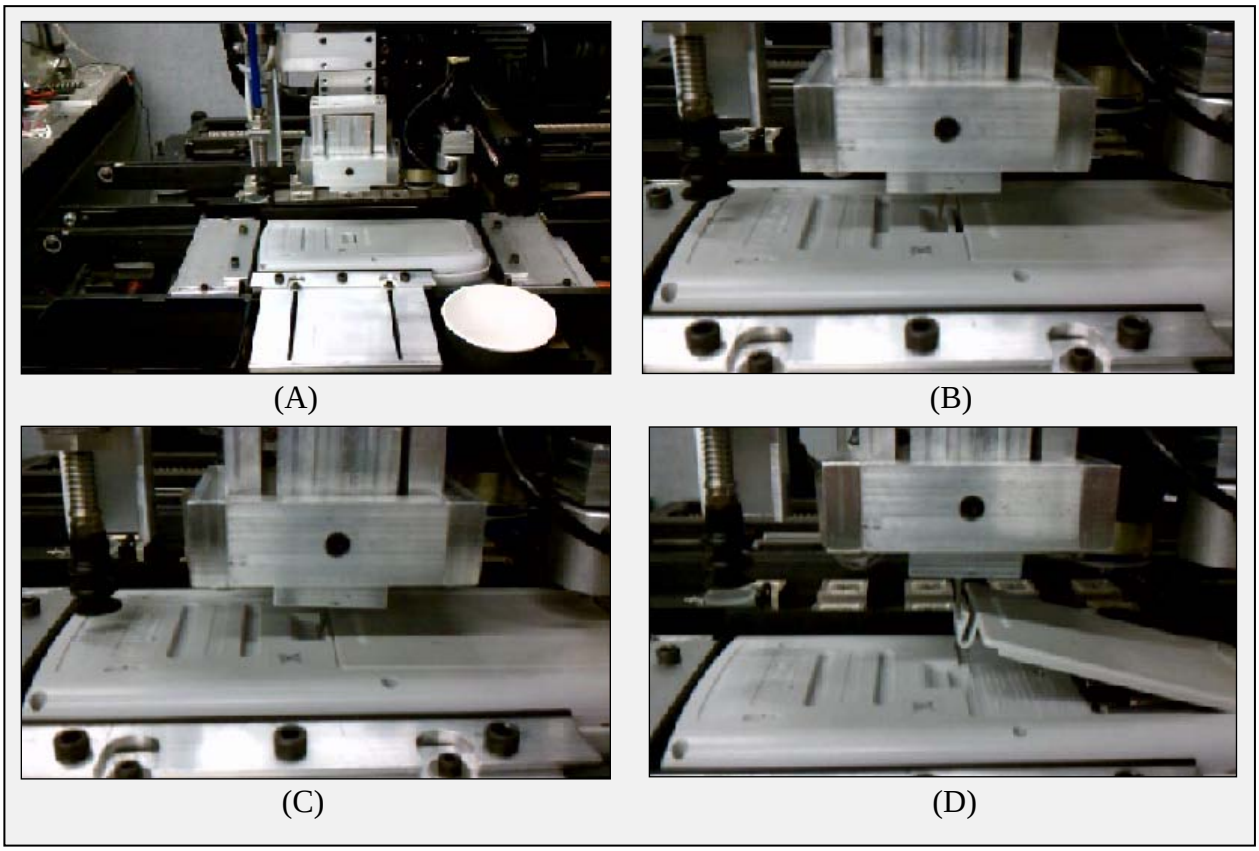

Figure 15: Snap-Fit Disassembly Routine

The next task is to remove the batteries. The batteries are released essentially the same way as the snap-fit. The tool tip is inserted against the edge of the battery opposite the spring. The battery is then pushed in the x-axis, compressing the spring. Once the force sensors indicate that the spring is fully compressed, the tool is moved up in the z-axis to release the battery. An electromagnet mounted on a pneumatic actuator is then used to retrieve the battery. The electromagnet is also equipped with a force sensor to indicate when it has made contact with the surface of the battery, at which point the pneumatic actuator is triggered up and the battery is lifted out of the device. The battery retrieval operations are illustrated in Figure 16. The system will continue to remove the batteries until they are all removed. The first battery was orientated so that the tool moved in the (+) x-direction ("right") to compress the spring, where as Figure 16(D) shows the second battery being released by moving the tool in the (-) x-direction ("left").

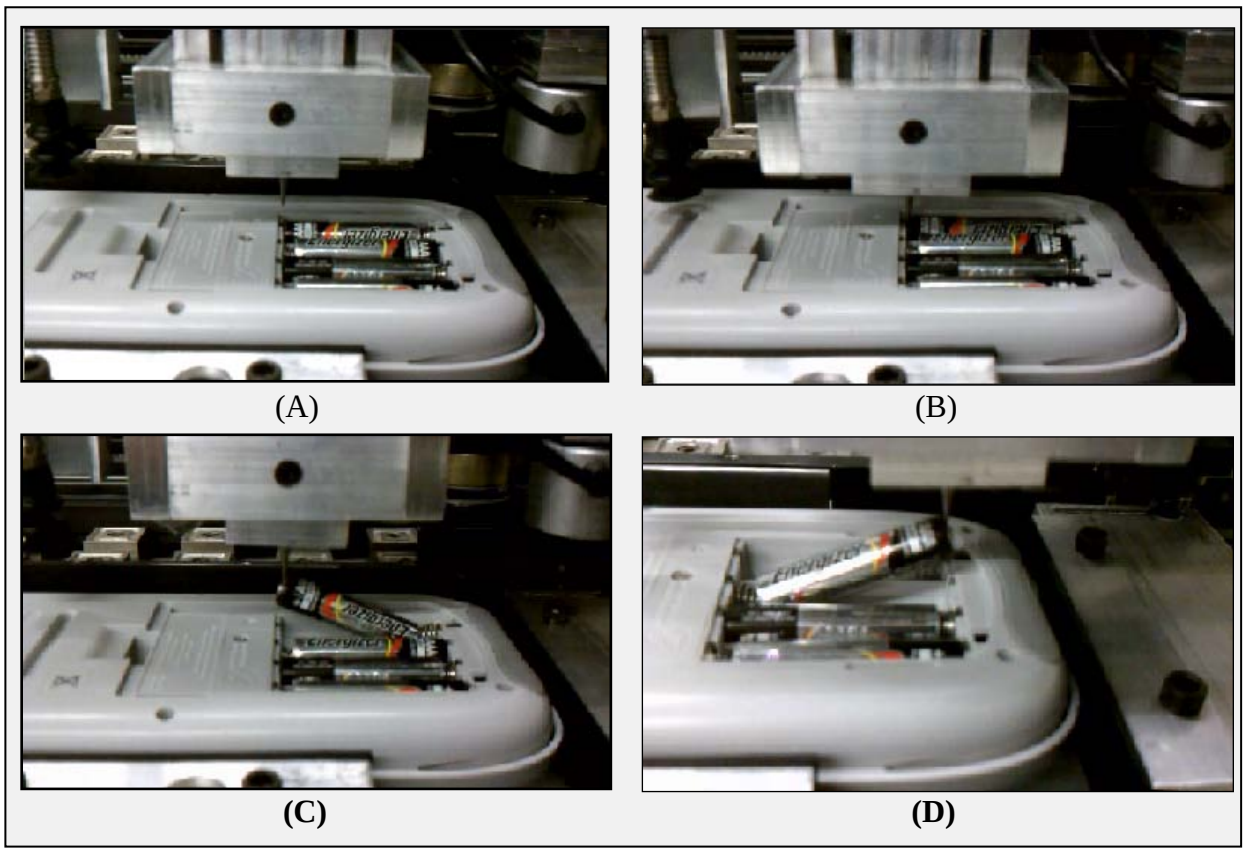

Figure 16: Battery Disassembly Routine

VI. Force Sensor Results

To demonstrate how the disassembly tool is controlled based on force sensor feedback, force sensor readings were recorded during the disassembly operations. The position feedback from the encoders was also recorded for the x, y, and z axes. In all of the following force plots, FSR1 corresponds to the force sensor that reads horizontal forces when the tool is moved "left" or along the negative x-axis, FSR2 corresponds to the force sensor that reads horizontal forces when the tool is moved "right" or along the positive x-axis, FSR3 corresponds to the force sensor that reads vertical forces applied to the tool tip along the z-axis, and FSR4 corresponds to the force sensor that reads vertical forces applied to the electromagnet along the z-axis.

The first disassembly operation analyzed is releasing a snap-fit with a "left" orientation as shown in Figures 17 and 18. The z-axis moves down quickly until it reaches the depth originally measured by the Kinect sensor and from that point slowly moves down until it comes into contact with the calculator surface. When the tool tip reaches the calculator surface, FSR3 measures the vertical force applied to the tool and z-axis motion is stopped as seen at approximately .35 seconds. The tool then moves to the left to deflect the snap-fit. As the tool tip presses the snap-fit lever, the force measured by FSR1 increases until it reaches the programmed threshold force 17.8 N (4.0 lbs) that indicates the snap-fit is fully deflected. When the threshold force is reached (t=0.7 sec), motion stops in the x-axis and the z-axis is moved up to release the snap-fit. While the z-axis moves up, the force measured by FSR1 decreases as the tool tip swings back to the neutral position. Once the force read by FSR1 is approximately zero (t=0.8 sec), the tool recognizes that the snap-fit has been successfully released and is ready for removal. After the snap-fit is released, the z-axis continues to move up to its zero position before the vacuum gripper is used to retrieve the snap-fit cover.

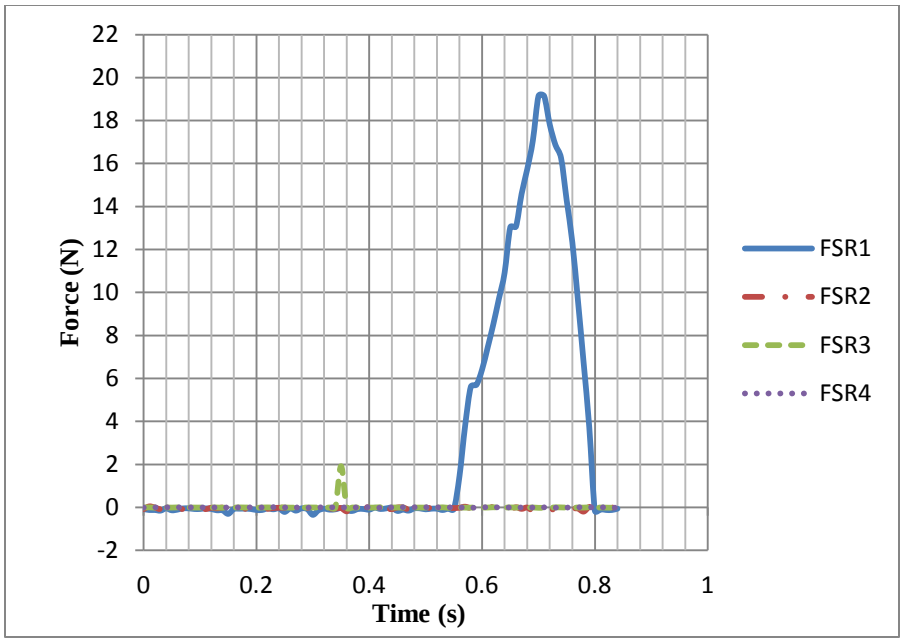

Figure 17: Force Response Plot for Snap-Fit with "Left" Orientation

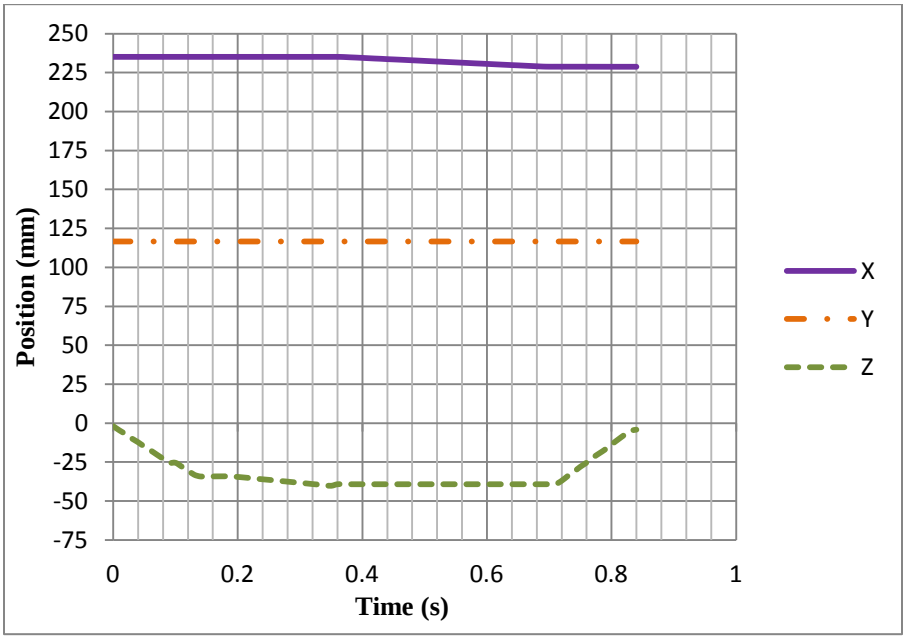

Figure 18: Position Plot for Snap-Fit with "Left" Orientation

The same adaptive force method is used to release a snap-fit with a “right” orientation as shown in Figures 19 and 20. In this case, however, FSR2 is the sensor that measures the force

applied to the tool tip as it presses the snap-fit. Note the similarity of the force profile for FSR1 (in Figure 17) and FSR2 (in Figure 19) which is an indication of the tool symmetric design.

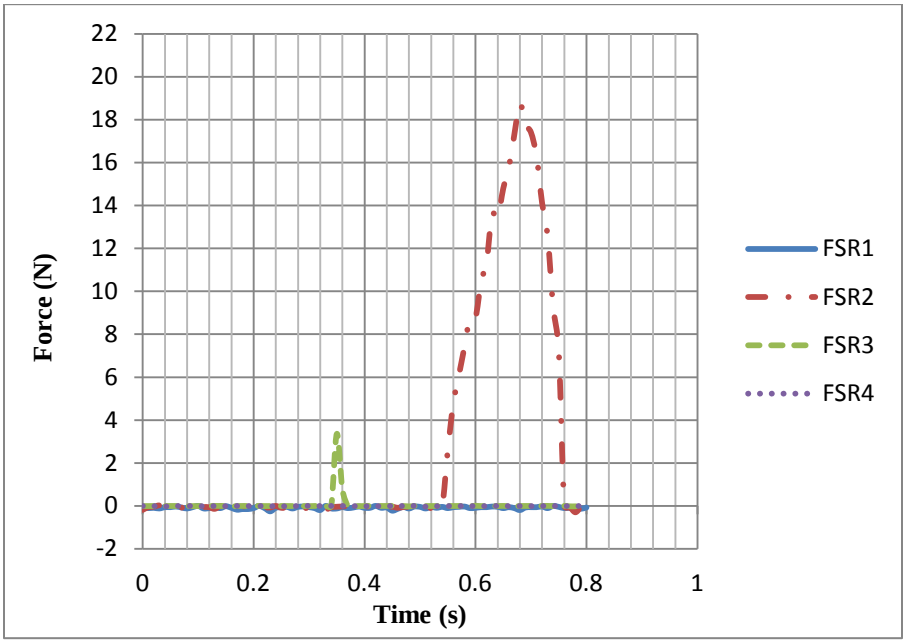

Figure 19: Force Response Plot for Snap-Fit with "Right" Orientation

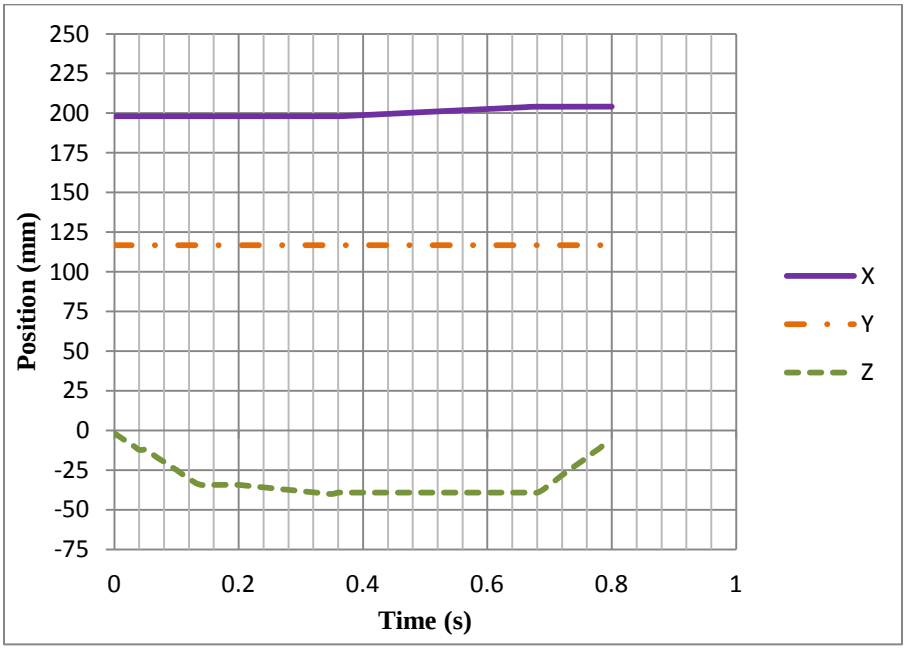

Figure 20: Position Plot for Snap-Fit with "Right" Orientation

The disassembly method used to release the batteries is similar to that used to unfasten the snap-fit. Thus, the force response plot for the batteries is also comparable to that of the snap-fit. Figures 21 and 22 show the interactions for the release of a battery with a “left” orientation. The z-axis is moved down to the edge of the battery opposite the spring until FSR3 reads a force applied to the tool tip in the vertical direction (t=0.4 sec). The tool is then moved left, pushing the battery and compressing the spring. Once FSR1 measures a force greater than the threshold force (19 N), motion on the x-axis stops and the z-axis is moved up to release the battery (t=0.6 sec). As one can see in Figure 21, FSR1 reaches a peak force slightly higher than the threshold force, which is due to a small delay between the force sensor signal and the command sent to stop motion in the x-axis. Once FSR1 indicates that the battery is successfully released, the x and y axes are moved to center the electromagnet over the battery (t=0.78 sec). After the pneumatic actuator is triggered, the z-axis is moved down until FSR4 measures a force applied on the electromagnet (t=1.16 sec). At this point the pneumatic actuator fires up, the z-axis is moved up, and the electromagnet carries the battery to its respective bin for disposal.

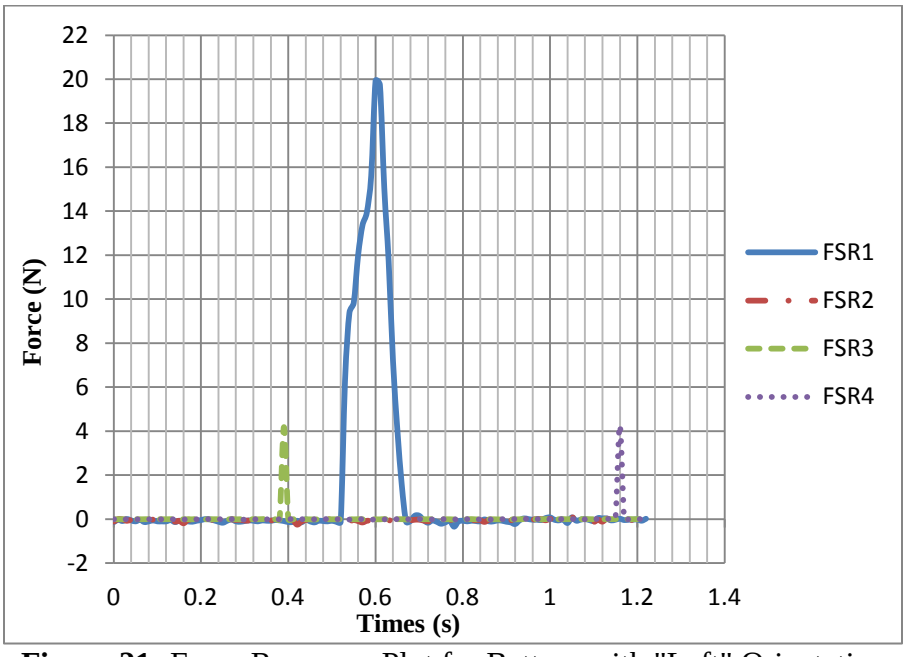

Figure 21: Force Response Plot for Battery with "Left" Orientation

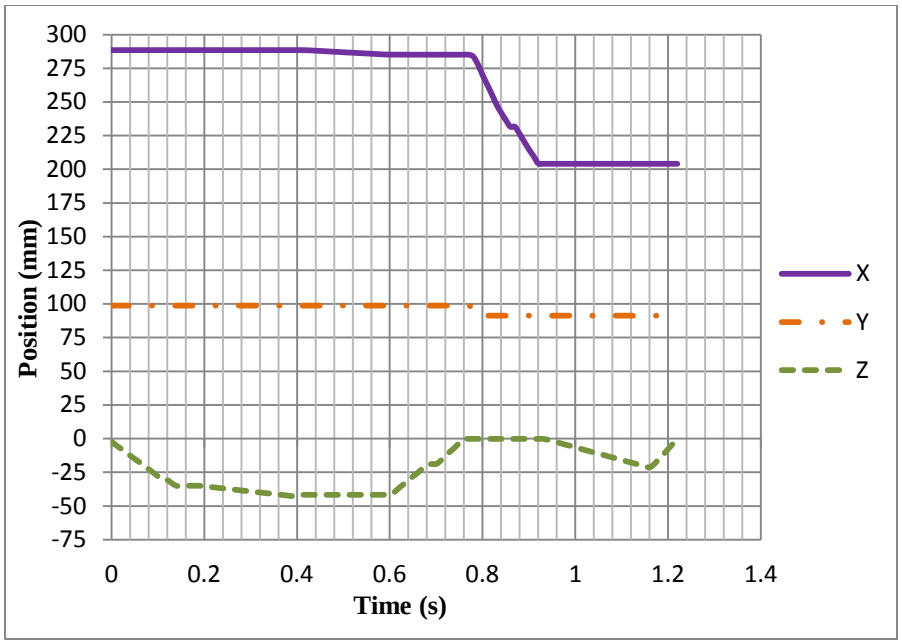

Figure 22: Position Plot for Battery with "Left" Orientation

The same approach was used to release a battery with a “right” orientation .In this case, however, FSR2 is the sensor that measures the force applied to the tool tip as it pushes the battery against the spring.

When the position of the device held in the vice is shifted in the x-y plane towards the edge of the image frame, small inaccuracies can occur in the device’s localization. Errors on the order of 1-2 pixels have been observed in the localization, which corresponds to approximately 0.889 mm – 1.905 mm in world coordinates. As a result, an error routine was developed to adapt to these small inaccuracies.

The error routine essentially checks to make sure the tool tip catches the appropriate edge of the battery and begins to push the battery against the spring. When the z-axis is moved down and detects a vertical force in the tool tip, the tool begins to move along the x-axis in the appropriate direction to compress the spring. However, at this point the tool is unaware if it actually touched down in the correct position. When the tool begins its movement in the x-axis

the distance it travels is recorded. If the tool moves more than 5.0 mm without detecting a horizontal force, the tool realizes it did not touch down in the correct position and moves back to readjust its start position. The tool tip moves up in the z-axis and then moves to a position offset 0.75 mm from the original start position along the x-axis in the direction opposite the motion of the tool. The tool tip then retries its attempt to release the battery from the new start position. The disassembly tool will make a maximum of three attempts to release any one battery. Figure 23 illustrates the performance of the error routine.

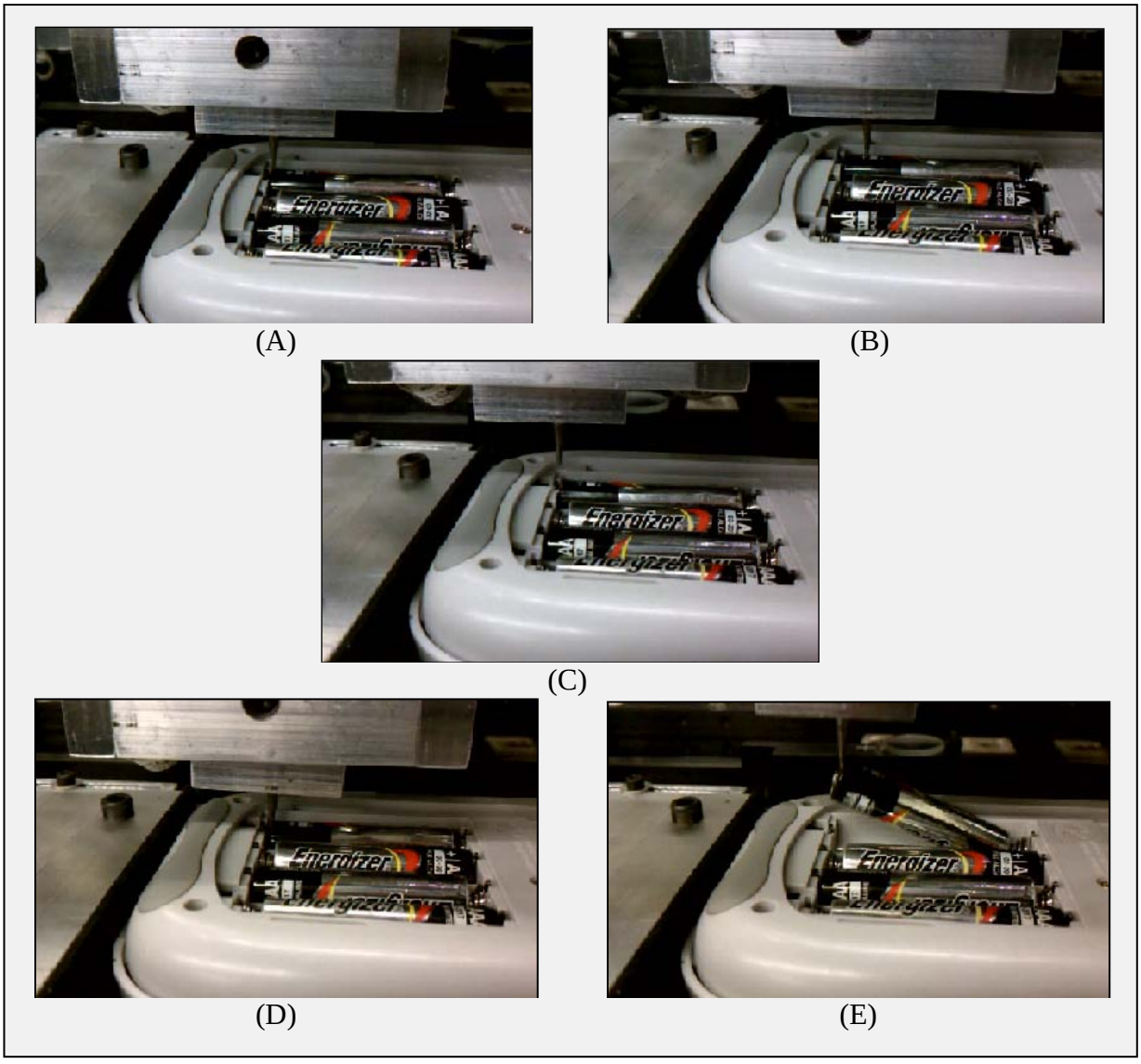

Figure 23: Battery Error Routine Illustration

Figures 24 and 25 depict the force interactions that occur during the execution of the error routine. As seen in Figure 24, FSR3 detects a vertical force on the tool tip (t=0.32 sec) and the x-axis begins to move in the positive x-direction. When FRS2 doesn't register a force, the tool moves in the negative x-direction (t=0.62sec) past its original starting position. The z-axis moves down again and registers a vertical force (t=0.92sec), signaling the tool to move in the positive x-direction. On this attempt, the force measured by FSR2 increases and indicates that the tool tip has caught the battery edge.

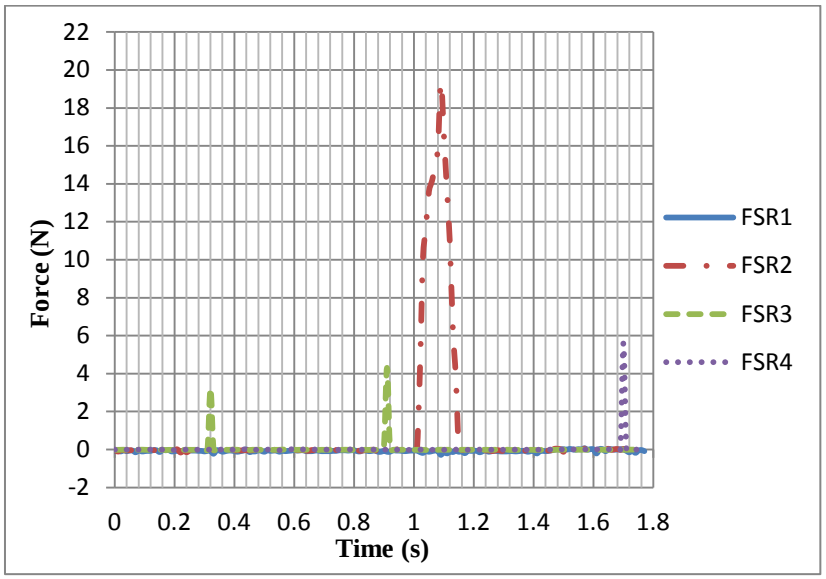

Figure 24: Force Response Plot for Battery Error Routine with "Right" Orientation

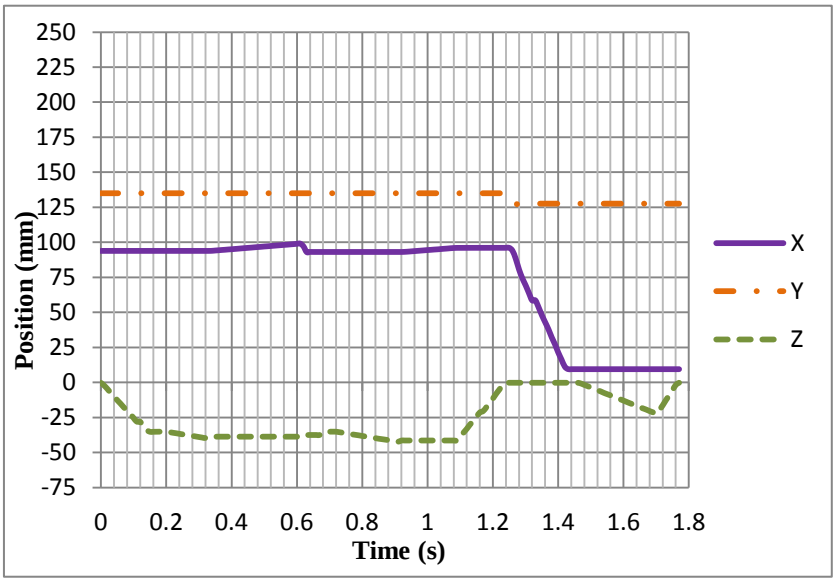

Figure 25: Position Plot for Battery Error Routine with "Right" Orientation

The error routine can also be used to detect if a battery is missing from an electronic device. The tool will still try to release a battery as if one was there, but after three failed attempts at catching a battery edge the tool will stop and prompt the user that an error has occurred releasing the battery. At this point, the user has the option to command the tool to move to the next battery or restart the disassembly routine.

VII. Internal Snap-fit Tool Tip

Another type of plastic snap-fit cover is common among the family of similar devices explored. Rather than an external U-shaped cantilever snap-fit, these battery covers use an internal cantilever snap-fit to fasten. These covers are removed by pushing down at the edge where the snap-fit is located and sliding the cover off. An example of this type of internal snap-fit fastener is pictured in Figures 26 and 27.

Figure 26: Internal Snap-Fit Cover

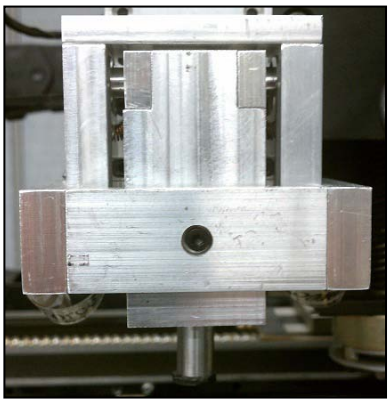

Figure 27: Internal Snap-Fit Tool Tip

An image of the new tool tip mounted on the disassembly tool is shown in Figure 27. Rather than the tapered design of the original tool tip, the new tool tip consists of a 3/8” diameter cylinder with a rubber pad attached to the surface. The increased surface area of the tool tip combined with the rubber pad provides the traction force necessary to slide and release the internal snap-fit cover.

The disassembly process implemented to remove the internal snap-fit cover using this new tool tip is shown in Figure 28. First, the tool tip is moved to the x-y position where the snap-

fit is located inside the cover. The tool tip is then moved down in the z-axis until the vertical force sensor indicates the tool tip is pressing down on the snap-fit cover. Then the disassembly tool is moved in the appropriate direction along the x-axis to slide the cover and release the internal snap-fit. Once the snap-fit is released, the disassembly tool is moved up on the z-axis to the zero position. The vacuum gripper is then used to retrieve and dispose of the snap-fit cover using the same strategy as in the original disassembly routine.

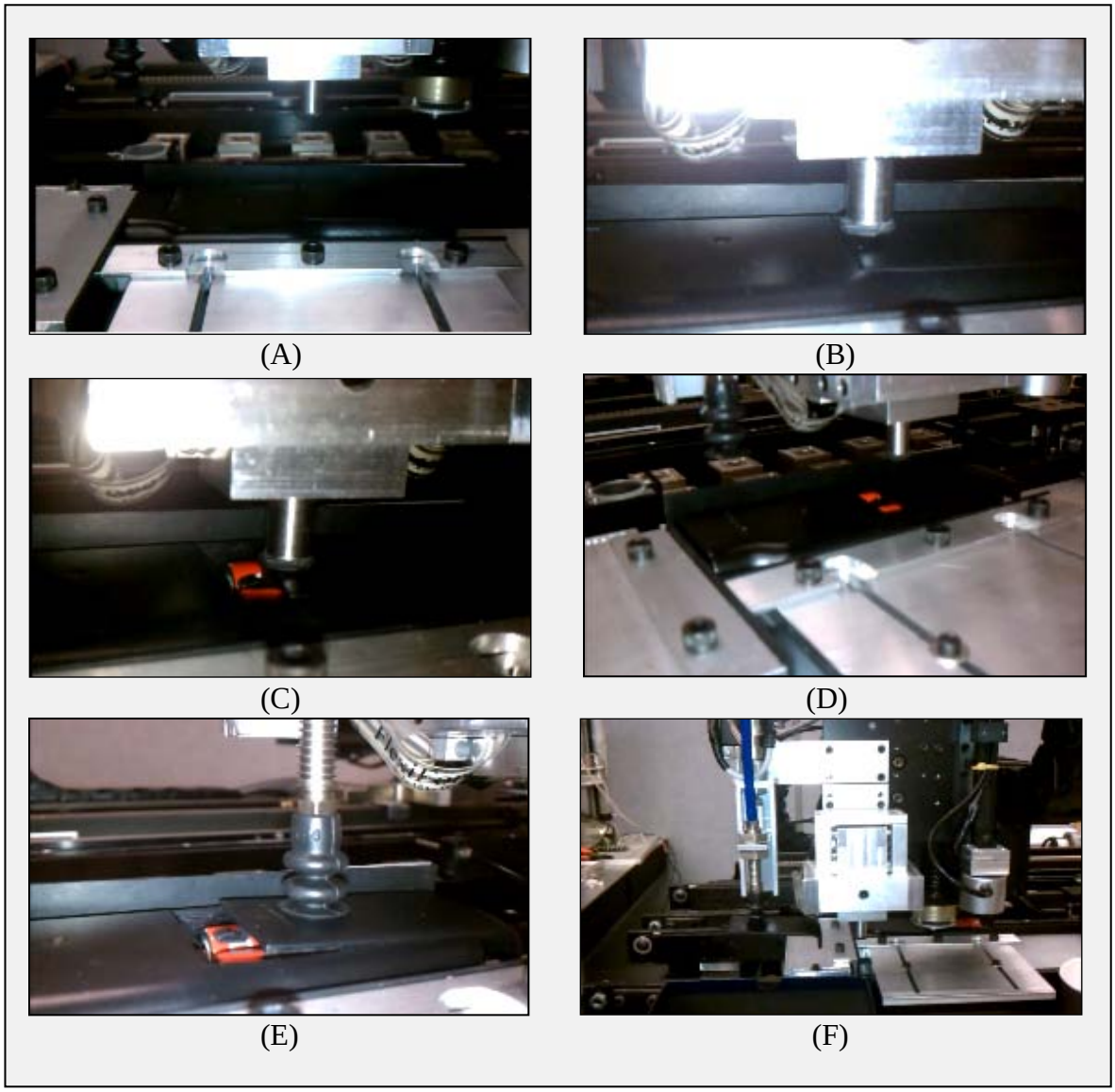

Figure 28: Internal Snap-Fit Disassembly Routine

The force response and position feedback of the disassembly tool during the release of the internal snap-fit cover are plotted in Figures 29 and 30 respectively.

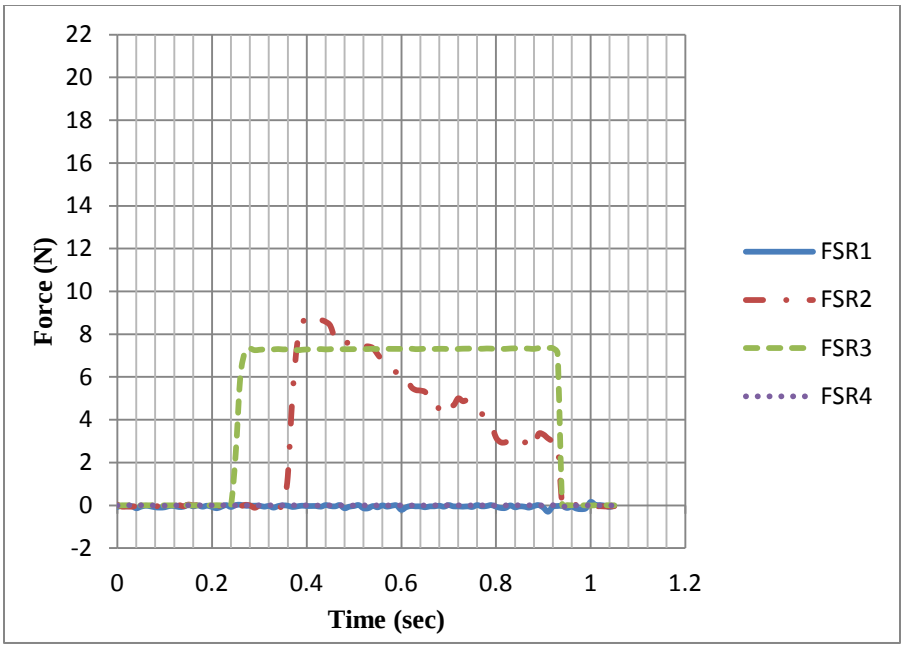

Figure 29: Force Plot for Internal Snap-Fit with "Right" Orientation

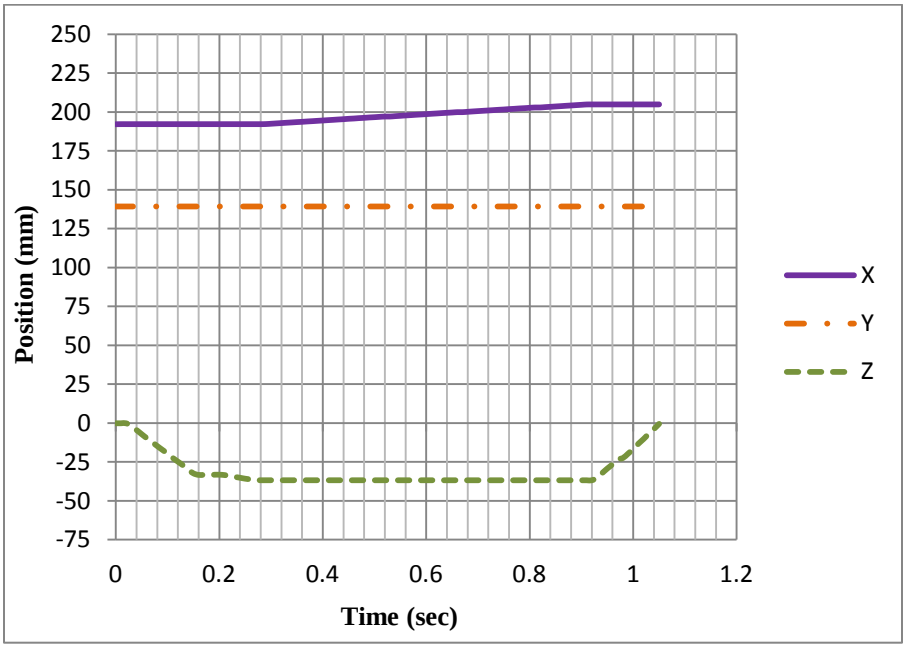

Figure 30: Position Plot for Internal Snap-Fit with "Right" Orientation

Figure 30 shows how the disassembly tool moves down in the z-axis once the tool tip is positioned at the snap-fit location (t=0.02 sec). The tool continues to move down until the tool tip presses down on the snap-fit cover with a force greater than 7 N, as indicated by FSR3 in Figure 29 (t=0.28 sec). After the threshold force is reached, motion stops in the z-axis and the tool moves 12.7 mm (0.5") in the positive x-direction because the snap-fit has a "right" orientation. As the tool moves along the x-axis, the snap-fit cover slides to the right and is released from the DVD remote housing. At this point, motion stops along the x-axis and the tool tip is moved up along the z-axis to the zero position (t=0.92 sec). When the tool moves up, the tool tip no longer contacts the cover's surface and the force read by FSR3 returns to zero. Also, when the disassembly tool is sliding the snap-fit cover in the x-direction, the moment arm rotates and applies a force at the "right" force sensor (FSR2). After the initial horizontal force is applied to unfasten the snap-fit, the force on FSR2 decreases as the snap-fit cover continues to slide to the right because less force is required to move the cover. Similar to FSR3, once the snap-fit cover is released and the tool is moved up in the z-direction, the force read by FSR2 quickly drops to zero as the moment arm swings back to the neutral position.

VIII. Conclusions

In this paper, a prototype automated disassembly tool was developed for to remove snap-fit covers and the batteries contained within. The design concept conceived to complete these tasks was a force sensing tool tip that uses force sensing resistors (FSRs) to approximate the values of forces applied to the tool tip. The use of FSRs resulted in a low-cost, flexible disassembly tool. By using the conductance of the FSR sensors, a linear model of the FSR output was calibrated to the force applied to the FSR. The force feedback from the FSRs was used to control the movement of the tool during disassembly operations. The disassembly tool was

mounted on the tool head module of a three-axis translational motion robot equipped with a pneumatically actuated vacuum gripper for the removal of the cover and an electromagnet for the removal of the batteries. An automated disassembly routine was programmed in which the robot was able to use the disassembly tool and recovery modules to perform the necessary disassembly operations to remove the snap-fit and batteries held within the device. The disassembly tool was tested on two electronic devices in various test configurations. Based on the success of the disassembly routine and the force sensor results for these test variations, it was concluded that the disassembly tool was able to react to forces applied at the tool tip and accomplish the required disassembly operations. Furthermore, the adaptability and ease of interface of the disassembly tool was also illustrated by the design of the additional tool tip used to successfully release internal snap-fit covers.

References

[1] B. Scholz-Reiter, H. Scharke, and A. Hucht, “Flexible robot-based disassembly cell for obsolete TV-sets and monitors,” *Robotics and Computer Integrated Manufacturing*, vol. 15, pp. 247–255, 1999.

[2] Weigl-Seitz, K. Hohm, M. Seitz, and H. Tolle, “On strategies and solutions for automated disassembly of electronic devices,” *The International Journal of Advanced Manufacturing Technology*, vol. 30, pp. 561–573, 2006.

[3] B. Basdere and G. Seliger, “Disassembly Factories for Electrical and Electronic Products To Recover Resources in Product and Material Cycles,” *Environmental Science Technologies*, vol. 37, no. 23, pp. 5354–5362, 2003.

[4] F. Torres, P. Gil, S. Puente, J. Pomares, and R. Aracil, "Automatic PC disassembly for component recovery," *The International Journal of Advanced Manufacturing Technology*, vol 23, pp. 39-46, 2004.

[5] U. Rebafka, G. Seliger, A. Stenzel, and B. Zuo, “Process model based development of disassembly tools,” *Proceedings of the Institution of Mechanical Engineers*, pp. 711–722, 2001.

[6] J. Park and G. Kim, “Development of the 6-axis force/moment sensor for an intelligent robot’s gripper,” *Sensors and Actuators A: Physical*, vol. 118, no. 1, pp. 127–134, 2005.

[7] K. Feldmann, S. Trautner, and O. Meedt, “Innovative disassembly strategies based on flexible partial destructive tools,” *In Proceedings of the IFAC Intelligent Assembly and Disassembly*, pp. 1–6, 1998.

[8] B. R. Zuo, A. Stenzel, and G. Seliger, “A novel disassembly tool with screwnail endeffectors,” *Journal of Intelligent Manufacturing*, vol. 13, no. 3, pp. 157–163, 2002.

[9] A. Weigl and M. Seitz, “Vision assisted disassembly using a dexterous hand-arm system: An example and experimental results,” in *Proc. IFAC Symp. Robot Control*, 1994, pp. 314–322.
[10] B. O’Shea, H. Kaebernick, S. S. Grewal, H. Perlewitz, K. Muller, and G. Seliger, “Method for automatic tool selection for disassembly planning,” *Assembly Automation*, vol. 19, no. 1, pp. 47–54, 1999.
[11] A. Elsayed, E. Kongar, S. Gupta, and T. Sobh."A Robotic-Driven Disassembly Sequence Generator for End-Of-Life Electronic Products," *Journal of Intelligent Robotics Systems*, vol. 68, no. 1, September 2012.
[12] A. Nikonovas, A. J. L. Harrison, S. Hoult, and D. Sammut, “The application of force-sensing resistor sensors for measuring forces developed by the human hand,” *Proceedings of the Institution of Mechanical Engineers, Part H: Journal of Engineering in Medicine*, vol. 218, no. 2, pp. 121–126, 2004.
[13] B. T. Smith, D. J. Coiro, R. Finson, R. R. Betz, and J. McCarthy, “Evaluation of force-sensing resistors for gait event detection to trigger electrical stimulation to improve walking in the child with cerebral palsy,” *Neural Systems and Rehabilitation Engineering, IEEE Transactions on*, vol. 10, no. 1, pp. 22–29, 2002.
[14] T. L. Glatt, *Controller apparatus using force sensing resistors*. US Patent # 5,515,044, Issued 1996.
[15] S. I. Yaniger and M. C. Pickett, *Force-sensing pointing device*. US Patent # 5,828,363, Issued 1998.
[16] C. A. Sellers, *Programmable multiple output force-sensing keyboard*. US Patent # 5,995,026, Issued 1999.
[17] W. B. Paley, *Three-dimensional mouse with tactile feedback*. US Patent # 5,506,605, Issued 1999.
[18] “Snap-fit Joints for Plastics.” Bayer Corporation, 2001.
[19] “Snap-Fit Design Manual.” Honeywell International Inc., 2002.
[20] “FlexiForce Sensors User Manual.” Tekscan, Inc., 2010.
[21] “FSR Integration Guide.” Interlink Electronics Sensor Technologies, 2010.
[22] P. Schumacher, “Design of a Tool for Automated Disassembly of Electronic Devices”, M.S. Thesis, University of Rhode Island, 2012.